

Magnetic order and disorder in a quasi-two-dimensional quantum Heisenberg antiferromagnet with randomized exchange

F. Xiao,^{1,2} W.J.A. Blackmore,³ B.M. Huddart,⁴ M. Gomilšek,^{5,4} T.J. Hicken,⁴

C. Baines,⁶ P.J. Baker,⁷ F.L. Pratt,⁷ S.J. Blundell,⁸ H. Lu,⁹ J. Singleton,⁹ D.

Gawryluk,¹⁰ M.M. Turnbull,¹¹ K.W. Krämer,² P.A. Goddard,^{3,*} and T. Lancaster^{4,†}

¹Laboratory for Neutron Scattering, Paul Scherrer Institut, CH-5232 Villigen PSI, Switzerland

²Department of Chemistry and Biochemistry, University of Bern, CH-3012 Bern, Switzerland

³Department of Physics, University of Warwick, Coventry, CV4 7AL, UK

⁴Durham University, Department of Physics, South Road, Durham, DH1 3LE, UK

⁵Jožef Stefan Institute, Jamova c. 39, SI-1000 Ljubljana, Slovenia

⁶Laboratory for Muon Spin Spectroscopy, Paul Scherrer Institut, CH-5232 Villigen PSI, Switzerland

⁷ISIS Pulsed Neutron and Muon Facility, STFC Rutherford Appleton Laboratory, Harwell Oxford, Didcot, OX11 0QX, UK

⁸Oxford University Department of Physics, Clarendon Laboratory, Parks Road, Oxford, OX1 3PU, United Kingdom

⁹NHML, Los Alamos National Laboratory, Los Alamos, NM 87545, USA

¹⁰Laboratory for Multiscale Materials Experiments,

Paul Scherrer Institut, CH-5232 Villigen PSI, Switzerland

¹¹Carlson School of Chemistry and Biochemistry and Department of Physics, Clark University, Worcester, Massachusetts 01610, USA

We present an investigation of the effect of randomizing exchange strengths in the $S = 1/2$ square lattice quasi-two-dimensional quantum Heisenberg antiferromagnet $(\text{QuinH})_2\text{Cu}(\text{Cl}_x\text{Br}_{1-x})_4 \cdot 2\text{H}_2\text{O}$ ($\text{QuinH} = \text{Quinolinium}, \text{C}_9\text{H}_8\text{N}^+$), with $0 \leq x \leq 1$. Pulsed-field magnetization measurements allow us to estimate an effective in-plane exchange strength J in a regime where exchange fosters short-range order, while the temperature T_N at which long range order (LRO) occurs is found using muon-spin relaxation, allowing us to construct a phase diagram for the series. We evaluate the effectiveness of disorder in suppressing T_N and the ordered moment size and find an extended disordered phase in the region $0.4 \lesssim x \lesssim 0.8$ where no magnetic order occurs, driven by quantum effects of the exchange randomness.

Understanding the role of disorder at a microscopic level on magnetic ground states is an important prerequisite to future applications of quantum spin systems. The ground states of unfrustrated magnets with classical moments are predicted to be robust with respect to low levels of disorder, while such disorder is thought to have a far stronger effect on quantum spin systems [1–5]. The two-dimensional (2D) $S = 1/2$ square lattice quantum Heisenberg antiferromagnet (QHAF) has previously been investigated in this context through the introduction of nonmagnetic on-site impurities in CuO [6] and CuF_4 [7–9] planes. However, there is less work on other forms of quenched disorder such as the case of randomized bonds, where the strength of exchange coupling is varied across the lattice. Numerical treatments of this problem [2] suggest that if the bond disorder is homogeneous, the ground state of the system is very robust, even against strong bond disorder, with the spin stiffness and order parameter being exponentially reduced and only vanishing in the case of infinite randomness. However, if disorder is inhomogeneous [3] the occurrence of lower-dimensional quantum states, such as dimer singlets, significantly enhances quantum fluctuations, which reflect low-temperature, time-dependence in the states of the system (and differ from the time-independent, temperature-driven classical fluctuations that dominate magnetism at elevated temperatures). Disorder can also

give rise to spin frustration, which strongly suppresses correlation lengths [4]. In these latter cases, long-range order can be destroyed with a quantum-disordered phase resulting [10]. We present here a rare and complete experimental investigation of a 2D QHAF with randomized exchange strengths. We indeed find evidence for the formation of small clusters of fluctuating quantum spins acting to destabilize magnetic order.

We use coordination chemistry to generate a tuneable family of low-dimensional materials in which $S = 1/2$ Cu^{2+} ions are linked magnetically via a superexchange pathway mediated by halogen bonds. Previous work has shown that by substituting halogen ions in the superexchange pathway, differing exchange strengths can be realised [11, 12]. For example, an investigation of one-dimensional $\text{Cu}(\text{py})_2(\text{Br}_{1-x}\text{Cl}_x)_2$ ($\text{py} = \text{pyridine}, \text{C}_5\text{H}_5\text{N}$) [13], showed that randomized bonds have a strong effect on the exchange energy J , ordering temperature T_N and sublattice magnetization m .

The square lattice case is addressed here through pulsed-field magnetization and muon-spin rotation ($\mu^+\text{SR}$) measurements of the series $(\text{QuinH})_2\text{Cu}(\text{Cl}_x\text{Br}_{1-x})_4 \cdot 2\text{H}_2\text{O}$ ($\text{QuinH} = \text{Quinolinium}, \text{C}_9\text{H}_8\text{N}^+$) [14–16]. This combination of techniques is well suited to determining the magnetic ground state of low-dimensional Cu^{2+} complexes [17–19]. Our series is based on 2D antiferromagnetic (AF) layers of CuZ_4^{2-}

distorted tetrahedra (where the halogen $Z = \text{Cl}$ or Br). The tetrahedra are related by C-centering, resulting in a square magnetic lattice, with each $S = 1/2 \text{ Cu}^{2+}$ ion having four identical nearest neighbours. Hydrogen bonding to water molecules within the layer generates close Z - Z contacts, providing the AF superexchange pathway. These 2D AF layers are well isolated owing to the presence of alternating layers of QuinH cations. The magnetic properties of the $x = 0$ compound $(\text{QuinH})_2\text{CuBr}_4 \cdot 2\text{H}_2\text{O}$ suggest it represents a good realization of the 2D QHAF model with intraplane exchange strength $J(x = 0) = 6.17(3) \text{ K}$ [15]. Comparing $x = 1$ ($Z = \text{Cl}$) and $x = 0$ ($Z = \text{Br}$) materials, there are differences of only 4% and 0.4% respectively in the distance between Cu^{2+} ions along the a -axis and b -axis. We expect that these differences will have a much smaller effect on the magnetism than that caused by the varying chemical composition of the superexchange pathways. Energy-dispersive X-ray spectroscopy (EDX) measurements [16] confirm that there is no macroscopic separation of Br- and Cl-rich structures.

To determine the effective intraplane exchange J , low-temperature ($T \approx 0.6 \text{ K}$) pulsed-field magnetization measurements were made on materials with $0 \leq x \leq 1$ (Fig. 1) as detailed in the Supplemental Information [16]. Magnetization measurements are made at $T \ll J$ where collective behaviour of the spins is expected. The magnetization M as a function of applied field for the $x = 0$ and 1 materials [Fig. 1(c)] shows a convex rise to saturation, indicative of 2D magnetic interactions [17]. Where sufficient correlations (promoted by a narrow distribution in J) are present (see below), saturation of M at applied field H_{sat} occurs via a sharp change in the slope of M , giving rise to a minimum in d^2M/dH^2 that allows H_{sat} to be determined. For $x = 0$, this occurs at $\mu_0 H_{\text{sat}} = 16.9(4) \text{ T}$, whereas for $x = 1$ we find $\mu_0 H_{\text{sat}} = 3.8(3) \text{ T}$ [Fig. 1(b) and (c)]. Within a mean-field approximation, saturation occurs when $g\mu_B\mu_0 H_{\text{sat}} = nJ$ [17] and $n = 4$ is the number of nearest neighbours in the 2D planes. Using the published value of $g = 2.15$ for the $x = 0$ material [15], this gives $J(x = 0) = 6.1(1) \text{ K}$, in good agreement with the previous estimate. Assuming a similar g -factor, a value of $J(x = 1) = 1.4(1) \text{ K}$ is obtained, consistent with previous measurements that suggest $J_{\text{Br}} \approx 4J_{\text{Cl}}$ for Cu^{2+} QHAFs [11].

For concentrations with $x \gtrsim 0$ we again measure the characteristic 2D convex rise to saturation, but this becomes less pronounced for $x \geq 0.05$ where the saturation field [and therefore $J(x)$] decreases and change in the slope of $M(H)$ becomes less sharp [Fig. 1 (d)]. As x is increased further towards $x \approx 0.4$, the approach to saturation broadens, such that the trough in d^2M/dH^2 is hard to discern [16]. However, a sharp elbow in $M(H)$ is still observed at the saturation field, which can be identified by extrapolation of the data above and below H_{sat} [Fig. 1(f)]. For $x = 0.57, 0.74$ and 0.84 there is no clear

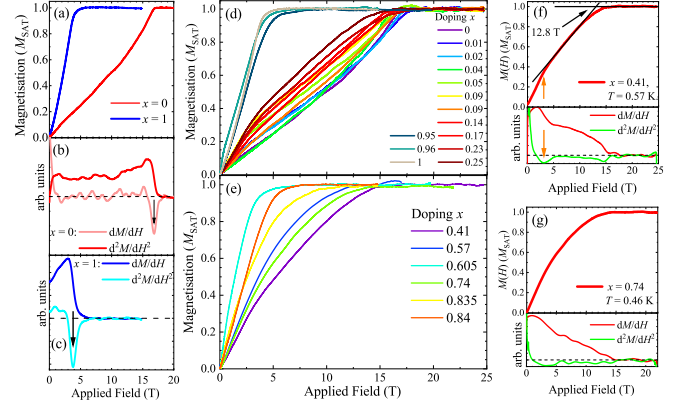


FIG. 1: Low-temperature ($T \approx 0.6 \text{ K}$) single-crystal magnetization data. (a)-(c) $M(H)$, dM/dH and d^2M/dH^2 for $x = 0$ and $x = 1$. (d) Low and high values of x show a sharp change in the slope of $M(H)$ at H_{sat} , but (e) intermediate values do not. Details of the data for (f) $x = 0.41$ and (g) $x = 0.74$. Black arrows indicate H_{sat} , orange arrow indicates the low-field kink feature.

feature in the $M(H)$ data [16] and it is not possible to estimate an effective value for J [Fig. 1(e) and (g)]. In this region $M(H)$ rises smoothly to saturation but cannot be fitted to a Brillouin function, suggesting that, while interactions between spins exist, correlations characterized by a single effective exchange energy are not present, or drop below a certain critical length scale. The sharp change in the slope of $M(H)$ at saturation becomes resolvable again for $x \geq 0.84$ and, as the concentration approaches $x = 1$, the traces develop the convex shape observed at low x . This is consistent with the return to 2D QHAF behavior in the $x = 1$ material.

We can assess the coherence length ξ required to give a resolvable transition in $M(H)$ through temperature-dependent pulsed-field measurements of the $x = 0$ compound between 0.5 and 15 K [16]. As T is raised, the saturation point becomes more rounded such that the width of the trough in d^2M/dH^2 increases and the amplitude decreases. For $T \gtrsim 4 \text{ K}$ it is no longer possible to clearly identify H_{sat} . The coherence length in square lattice planes can be estimated using $\xi/d \approx 0.498(10.44T/J)\exp(1.131J/T)$ where d is the magnetic lattice parameter [20], which holds for $H = 0$ and $T \ll J$. Coupling this formula with the limiting value of T , above which H_{sat} is undefined, suggests that the magnitude of exchange can be identified only when $\xi/d \gtrsim 2$ at $H = 0$.

In addition to the feature at saturation, the $M(H)$ data for some samples show a kink at fields considerably lower than H_{sat} for the $x = 1$ system. The kink is resolvable [Fig. 1(d)] for x between 0.05 and 0.61 [16], indicated by an orange arrow in Fig. 1(f). We attribute this to the presence of isolated clusters of spins (e.g. dimers, trimers, square plaquettes, etc.) coupled by Cl-Cl halogen exchange bonds, which are weaker than Br-Br bonds

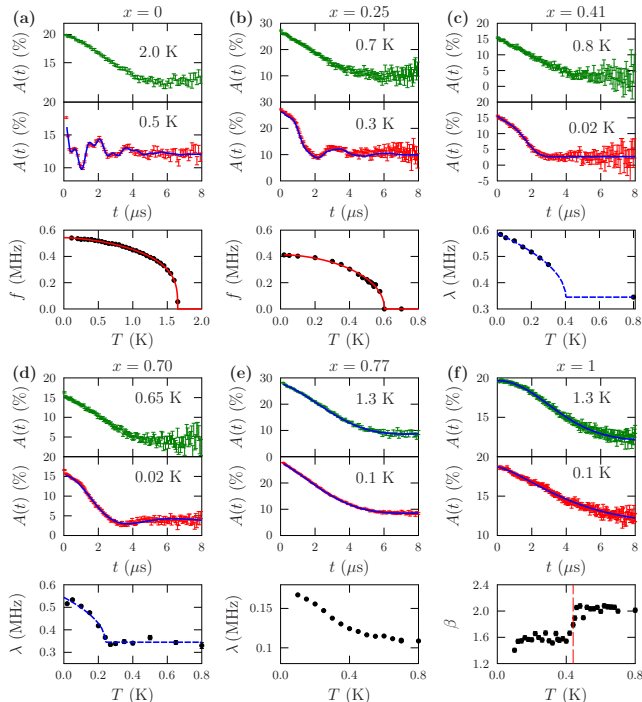


FIG. 2: Results of ZF μ^+ SR measurements. (a-f) *Top*: Example high-temperature spectra; *Middle*: example low-temperature spectra; *Bottom*: oscillation frequency ν , relaxation rate λ or shape parameter β .

and thus easier to saturate with an applied field. (The effect of these localized units is discussed below.)

Although the 2D QHAF should only show long-range magnetic order (LRO) at $T = 0$, in any realization of the model in a three-dimensional material the presence of interplane exchange J_\perp leads to a transition with $T_N > 0$. To determine T_N , zero-field (ZF) μ^+ SR measurements were made [21, 22]. Oscillations in the asymmetry are observed in some members of the series at low T (Fig. 2), providing unambiguous evidence of LRO. For materials with $x \leq 0.25$ oscillations are observed at multiple (2 or 3) frequencies ν_i [Fig. 2(a,b)] consistent with several magnetically inequivalent muon sites. We find $T_N(x=0) = 1.65(1)$ K, and transition temperatures that decrease smoothly with increasing x ; $T_N(x) = 0$ extrapolates to zero at $x \approx 0.35$. The frequency $\nu_i(T \rightarrow 0)$ is proportional to the moment size on the Cu^{2+} ions and hence to the sublattice magnetization m . We measure relatively small frequencies compared to typical 3D systems, reflecting a reduced ordered moment (expected to be $0.33\mu_B$ for $T \rightarrow 0$ in spin wave theory [23]). These frequencies decrease with increasing x with m dropping by around 24% from $x = 0$ to 0.25.

The behaviour is qualitatively different for samples with $0.41 \leq x \leq 0.77$ [Fig. 2(c,d,e)] where no oscillations are resolved down to 0.02 K. Instead, spectra resemble a distorted Kubo-Toyabe (KT) function at low T

[22], corresponding to disordered quasistatic moments in the materials, with the distortion to the spectra likely reflecting short-range order along with some limited dynamic fluctuations. As T is increased, the spectra change such that they resemble dynamic, exponential functions above $x \gtrsim 0.5$ K. These data can be parametrized using a stretched-exponential envelope function $e^{-(\lambda t)^\beta}$ that accounts for the early time behaviour of the spectra. The transition between the static and dynamic regimes appears abrupt in the $x = 0.70$ sample, taking place at a freezing temperature to a glassy configuration around $T_f = 0.27$ K, with a similarly rapid variation in relaxation rate seen in $x = 0.41$ at low temperature, suggesting $T_f \approx 0.41$ K. No such sharp freezing is seen in the $x = 0.77$ sample, where the relaxation rate λ drops fairly smoothly with increasing T (with a change in slope around 0.4 K, likely related to the freezing seen in other concentrations).

The observed behavior is qualitatively different again in the $x = 0.89$ and $x = 1$ materials [Fig. 2(f)] where an abrupt transition to LRO takes place with similar T_N . This is seen via μ^+ SR oscillations at a single characteristic frequency in the $x = 0.89$ material and via the β parameter in the $x = 1$ material, where oscillations occur only with low amplitude. We are therefore able to assign $T_N(x=1) = 0.44(1)$ K. It is notable that the oscillations in the $x = 0.89$ material are well described by a Bessel function, typical of incommensurate magnetic order [22]. The presence of incommensurate order might also be consistent with measured data for $0.1 \leq x < 0.41$ where non-zero phase offsets are observed in the oscillatory components, although the presence of multiple characteristic frequencies complicates the modelling of this feature.

At $x = 0$, we have $T_N/J = 0.27(2)$, which combined with predictions from Quantum Monte Carlo (QMC) simulations [24], suggests $|J_\perp/J| \approx 3.2 \times 10^{-3}$, indicating well-isolated magnetic layers. At $x = 1$ we observe magnetic order with $T_N/J = 0.31(2)$ and thus $|J_\perp/J| \approx 7.5 \times 10^{-3}$. Comparing, we have $J_\perp(x=1) = 0.014(5)$ K and $J_\perp(x=0) = 0.011(8)$ K, the same within uncertainties, demonstrating that the degree of isolation of the 2D layers is largely unaffected by substitution of Br for Cl. This implies that $J_\perp(0 < x < 1)$ is likely close to these values, and that the magnetic effects of bond randomness are attributable solely to disorder in the 2D layers.

A notional phase diagram for the system is shown in Fig. 3. The parameter x represents the fraction of Cl in a square 2D unit cell. Since halogen bonds are formed from two Z ions, the presence of Cl can create a Cl-Cl exchange bond [expected to be around 4 times weaker than Br-Br bond exchange based on the size of $J(x)$] or a mixed Cl-Br bond. The exchange J extracted from the $M(H)$ data provides the energy scale below which we would expect short-range AF correlations in 2D planes to dominate the magnetic behaviour for $T_N \ll T \ll J$. The

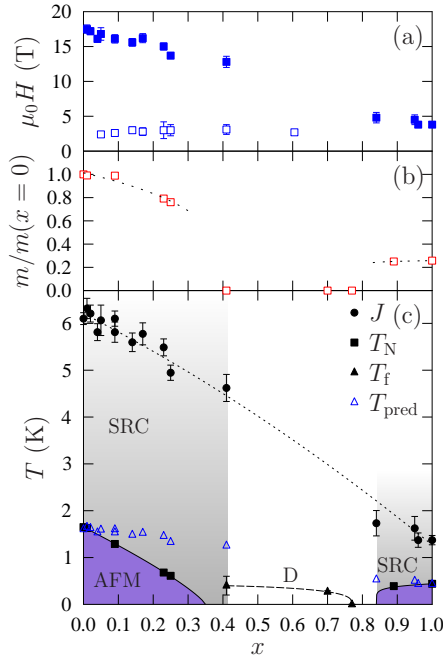


FIG. 3: (a) Fields at which $\mu_0 H_{\text{sat}}$ (filled symbols) and low-field kink (open symbols) are observed. (b) Evolution of estimated ordered moment with x . (c) Notional phase diagram showing antiferromagnetically ordered (AFM), short-range correlated (SRC) and disordered (D) regions. Open triangles show the predicted ordering temperatures from QMC assuming $J_{\perp} = 0.011$ K. Dotted line described in main text.

phase diagram is not symmetrical about $x = 0.5$ because x does not merely lead to random substitution but also decreases the effective value of J across the series.

We expect the effective exchange J through Z - Z contacts to reflect the size and shape of the orbitals [16]. The extracted values of $J(x)$ show a gradual decrease up to $x = 0.41$. This is also the region where LRO is observed, with T_N showing similar gradient to $J(x)$. If we combine the measured $J(x)$ with our estimated J_{\perp} we can use the QMC results [24] to predict values of T_N , shown by the unfilled triangles in Fig. 3. The measured T_N are seen to depart significantly from these predictions, showing that disorder has a strong effect in suppressing T_N beyond simply the gradual reduction in effective J . The ordered moment is seen to decrease as shown in Fig. 3(b). The behaviour in this part of the phase diagram is reminiscent of that for substitutional disorder in $\text{La}_2\text{Cu}_{1-z}(\text{Zn},\text{Mg})_z\text{O}_4$ [6]. In that case a fairly linear decrease was observed in T_N and m_s and a disappearance of LRO around 0.41. There is also a resemblance to the 1D molecular case in Ref. [13] where J values change approximately linearly across the phase diagram, while T_N and ordered moments drop rapidly on the Br-rich side of the phase diagram. In our case, the energy scales close to $x = 1$ are all lower owing to a smaller J mediated by the Cl ions. In the region, $0.84 \leq x \leq 1$ there is a

sufficient correlation length to identify J from the $M(H)$ data and LRO is restored above $x = 0.89$. However, T_N does not show the rapid decrease seen on the other side of the phase diagram when moving away from the pristine composition, likely because enhanced disorder is accompanied by an increase in effective J .

In the region $0.41 \leq x \leq 0.84$ the magnetic behaviour is more complicated. No LRO can be identified from the $\mu^+\text{SR}$ data across the entire region. The lack of a sharp feature in the $M(H)$ at saturation implies that collective behaviour characterized by a single effective exchange J is no longer straightforwardly applicable and that there is therefore a highly magnetically disordered region. Here we see evidence from $\mu^+\text{SR}$ for slow fluctuations of the spins for $T \gtrsim 0.5$ K with these becoming more static at the lowest measured T , although still not long-range ordered down to 0.02 K. The lack of muon oscillations in the static regime points to a coherence length $\xi/d \ll 10$ [22]. Non-zero M at small applied field implies that this disordered phase is not characterized by an energy gap. For samples with $0.41 \leq x \leq 0.7$ there is also evidence for a freezing of spins at low T . This would appear to suggest freezing of glassy behaviour in this region, as might be expected for a system forming clusters of strongly interacting spins surrounded by disordered moments [25].

We consider here three potential effects driving the form of the phase diagram: (i) percolation; (ii) bond energetics and (iii) quantum fluctuations. The bond percolation threshold for a square lattice is [26] $p_c = 1/2$. However, for our materials a single exchange bond comprises two possible substitution sites. If a single substitution per bond suffices to destabilize magnetic order then we should equate the percolation threshold p_c to the probability that one or more substitutions occurs on a single exchange bond $p_c = 1 - (1 - x_{c1})^2$, which gives a lower critical substitution level $x_{c1} = 0.29$, while at high x , we should have $p_c = 1 - x_{c2}^2$, which gives an upper critical substitution level $x_{c2} = 1 - x_{c1} = 0.71$. This could be compatible with the data for $x < 0.41$, but fails to describe the large- x behavior. Furthermore, it is unlikely that percolation is the sole driver of the observed behaviour since we are changing the strengths of random bonds, rather than removing exchange pathways.

An approximate criterion for the collapse of magnetic order (which could be short range) might be when the total exchange energy of the substituted bonds becomes larger than that of the unsubstituted bonds. We would expect a lower critical substitution level $x = x_{c1}$ to be determined by Br-Cl and Cl-Cl bonds acting as disorder in a Br-Br ordered background such that $(1 - x_{c1})^2 J_{\text{Br-Br}} = 2x(1 - x_{c1})J_{\text{Br-Cl}} + x_{c1}^2 J_{\text{Cl-Cl}}$. The upper critical substitution level $x = x_{c2}$ is then determined by Br-Cl and Br-Br bonds acting as disorder in a Cl-Cl ordered background giving $x_{c2}^2 J_{\text{Cl-Cl}} = 2x(1 - x_{c2})J_{\text{Br-Cl}} + (1 - x_{c2}^2)J_{\text{Br-Br}}$. The unknown exchange strength $J_{\text{Br-Cl}}$ can be determined by fitting the measured $J(x)$ with

$J(x) = (1-x)^2 J_{\text{Br-Br}} + 2x(1-x)J_{\text{Br-Cl}} + x^2 J_{\text{Cl-Cl}}$, which describes the data well [dotted line, Fig. 3(c)] and gives estimates $J_{\text{Br-Br}} = 6.2(1)$ K, $J_{\text{Br-Cl}} = 4.3(3)$ K, and $J_{\text{Cl-Cl}} = 1.3(1)$ K. These yield the critical substitution levels $x_{c1} = 0.40(2)$ and $x_{c2} = 0.88(2)$, both of which agree with the location of the collapse of magnetic order. In fact, values of x_c compatible with experiment result from a limited range of choices for $J_{\text{Br-Cl}}/J_{\text{Br-Cl}}$ [16].

Finally, theory predicts that the disorder-driven introduction of antiferromagnetically-coupled dimers, chains or other clusters acts to enhance quantum fluctuations, destroying magnetic order [3]. This scenario is consistent with our observations: the presence of the low-field kink in our magnetometry data points to high densities of microscopic clusters of Cu moments coupled by Cl bonds, while our EDX measurements showed no evidence for phase separation, suggesting inhomogeneities are limited to a local level. Calculations indeed show [16] that a random distribution of disordered bonds leads to a large concentration of dimers and trimers around $x = 0.2$, where we see T_N being strongly suppressed towards disorder.

In summary, we have performed a complete experimental investigation of the effect of bond substitution in the 2D QHAF. On adding small amounts of disorder to the pristine materials we find that regions of the sample remain correlated with a single effective value of J , which decreases as x increases. At the same time there is a preponderance for the formation of minority clusters (e.g. dimers and trimers) that enhance quantum fluctuations and act to suppress T_N more than is predicted from the change in J alone. There is evidence that LRO is incommensurate in nature. For high levels of disorder ($0.41 \leq x \leq 0.84$), while spins continue to interact, the highly correlated regions are no longer apparent, LRO is completely absent and spin freezing is evident. The critical substitution levels can be explained using arguments based on bond energetics.

Part of this work was carried out at SμS, Paul Scherrer Institut, Switzerland and STFC-ISIS Facility, Rutherford Appleton Laboratory, UK. We are grateful to EPSRC (UK) for financial support. This project is supported by the European Research Council (ERC) under the European Unions Horizon 2020 research and innovation program (Grant Agreement No. 681260). FX thanks C.P. Landee for inspiring discussion and B. Frey for assistance with EDX measurements in Bern. WJAB thanks the EPSRC for additional funding. Work at the National High Magnetic Field Laboratory is supported by NSF Cooperative Agreements No. DMR-1157490 and No. DMR-1644779, the State of Florida, the US DOE, and the DOE Basic Energy Science Field Work Project Science in 100 T. The financial support by the Swiss National Science Foundation under grant no. 200020_172659 is gratefully acknowledged. MG thanks the Slovenian Research Agency for additional funding under project No. Z1-1852. Data presented here will be made available via

Durham Collections.

* Electronic address: p.goddard@warwick.ac.uk

† Electronic address: tom.lancaster@durham.ac.uk

- [1] A.W. Sandvik, Phys. Rev. B **66**, 024418 (2002).
- [2] N. Laflorencie, S. Wessel, A. Läuchli, and H. Rieger, Phys. Rev. B **73**, 060403(R) (2006).
- [3] R. Yu, T. Roscilde and S. Haas, Phys. Rev. B **73**, 064406 (2006).
- [4] S. Liu and A. L. Chernyshev, Phys. Rev. B **87**, 064415 (2013).
- [5] The distinction between classical and quantum in this context rests on whether the properties of the system can be described using magnetic moments free to point in any direction, or if the quantization of spin component must be considered.
- [6] O. P. Vajk, P. K. Mang, M. Greven, P. M. Gehring, and J. W. Lynn, Science **295**, 1691 (2002).
- [7] V. Wagner and U. Kray, Z. Physik B **30**, 367 (1978).
- [8] Y. Okuda, Y. Tohi, I. Yamada and T. Haseda, J. Phys. Soc. Jpn. **49**, 936 (1980).
- [9] C. Binek and W. Kleemann, Phys. Rev. B **51**, 12888 (1995).
- [10] H. Kawamura and K. Uematsu, J. Phys.: Condens. Matter **31**, 50 (2019).
- [11] J.A. Schlueter, H. Park, G.J. Halder, W.R. Armand, C. Dunmars, K.W. Chapman, J.L. Manson, J. Singleton, R. McDonald, A. Plonczak, J. Kang, C. Lee, M.-H. Whangbo, T. Lancaster, A.J. Steele, I. Franke, J.D. Wright, S.J. Blundell, F.L. Pratt, J. deGeorge, M.M. Turnbull, and C.P. Landee, Inorg. Chem. **51**, 2121 (2012).
- [12] J. Liu, P. A. Goddard, J. Singleton, J. Brambleby, F. Foronda, S. J. Blundell, T. Lancaster, F. Xiao, R. C. Williams, F. L. Pratt, P. J. Baker, J. S. Möller, Y. Kohama, S. Ghannadzadeh, A. Ardavan, K. Wierschem, S. H. Lapidus, K. H. Stone, P. W. Stephens, J. Bendix, T. J. Woods, K. E. Carreiro, H. E. Tran, C. J. Villa, and J. L. Manson, Inorg. Chem **55**, 3515 (2016).
- [13] M. Thede, F. Xiao, Ch. Baines, C. Landee, E. Morenzoni, and A. Zheludev Phys. Rev. B **86**, 180407(R) (2012).
- [14] D.E. Lynch and I McClenaghan, Acta. Crystallogr. E **58**, m551 (2002).
- [15] R. T. Butcher, M.M. Turnbull, C.P. Landee, A. Shapiro, F. Xiao, D. Garrett, W.T. Robinson and B. Twamley, Inorg. Chem. **49**, 427 (2010).
- [16] Supplementary information contains descriptions of the of the material preparation, structure, experimental methods and further data on each composition measured, along with the results of simulations.
- [17] P. A. Goddard, J. Singleton, P. Sengupta, R. D. McDonald, T. Lancaster, S. J. Blundell, F. L. Pratt, S. Cox, N. Harrison, J. L. Manson, H. I. Southerland and J. A. Schlueter, New J. Phys. **10**, 083025 (2008).
- [18] P. A. Goddard, J. Singleton, I. Franke, J. S. Moller, T. Lancaster, A. J. Steele, C. V. Topping, S. J. Blundell, F. L. Pratt, C. Baines, J. Bendix, R. D. McDonald, J. Brambleby, M. R. Lees, S. H. Lapidus, P. W. Stephens, B. W. Twamley, M. M. Conner, K. Funk, J. F. Corbey, H. E. Tran, J. A. Schlueter, and J. L. Manson, Phys.

- Rev. B **93**, 094430 (2016).
- [19] F. M. Woodward, A. S. Albrecht, C. M. Wynn, C. P. Landee, and M. M. Turnbull, Phys. Rev. B **65**, 144412 (2002)
 - [20] P. Hasenfratz and F. Niedermayer, Phys. Lett. B **268**, 231 (1991); B. B. Beard, R. J. Birgeneau, M. Greven, and U.-J. Wiese, Phys. Rev. Lett. **80**, 1742 (1998); M. A. Kastner, R. J. Birgeneau, G. Shirane, and Y. Endoh, Rev. Mod. Phys. **70**, 897 (1998).
 - [21] S.J. Blundell, Contemp. Phys. **40**, 175 (1999).
 - [22] A. Yaouanc and P. Dalmat de Reotier *Muon Spin Rotation, Relaxation, and Resonance* (Oxford: OUP) (2010).
 - [23] E. Manousakis, Rev. Mod. Phys. **63**, 1 (1991).
 - [24] C. Yasuda, S. Todo, K. Hukushima, F. Alet, M. Keller, M. Troyer, and H. Takayama, Phys. Rev. Lett. **94**, 217201 (2005).
 - [25] K. Binder and A.P. Young, Rev. Mod. Phys. **58**, 801 (1986).
 - [26] D. Stauffer and A. Aharony *Introduction to Percolation Theory* (Taylor and Francis, London) (1991).